UDK 669.14.018.8:620.191
Original scientific article/Izvirni znanstveni članek

ISSN 1580-2949
MTAEC9, 43(3)137(2009)

THE OXIDATION OF DUPLEX STAINLESS STEEL AT MODERATELY ELEVATED TEMPERATURES

OKSIDACIJA DUPLEKSNEGA NERJAVNEGA JEKLA PRI ZMERNO POVIŠANIH TEMPERATURAH

Črtomir Donik, Aleksandra Kocijan, Irena Paulin, Monika Jenko

Institute of Metals and Technology, Lepi pot 11, SI-1000 Ljubljana, Slovenia
crtomir.donik@imt.si

Prejem rokopisa – received: 2009-03-17; sprejem za objavo – accepted for publication: 2009-05-04

The surface oxidation of DSS 2205 duplex stainless steel was studied by X-ray photoelectron spectroscopy (XPS). Two different techniques were used to produce thin oxide layers on polished and sputter-cleaned duplex stainless-steel samples. These samples were exposed to a 10^{-5} mbar pressure of pure oxygen inside the vacuum chamber and oxidized with an oxygen plasma from room temperature up to 300 °C. The experiments were made with the alloy after a controlled oxidation with oxygen atoms created in an inductively coupled plasma. The experiments were performed in the temperature interval from room temperature up to 300 °C. The compositions of the modified oxidized surfaces were determined from the XPS survey scans, and the chemistry of selected elements from the higher-energy-resolution scans of the appropriate peaks. Various Fe/Cr oxidized layers and various oxide thicknesses were observed and correlated with the temperature. It was found that all the techniques produced oxide layers with various traces of metallic components and with the maximum concentration of chromium oxide and iron oxide in layers close to the oxide-layer–bulk-metal interface.

Key words: duplex stainless steel, oxidation, plasma oxidation, XPS, stainless steel

Z rentgensko fotoelektronsko spektorskopijo (XPS) smo raziskovali površinsko oksidacijo dupleksnega nerjavnega jekla DSS 2205. Z željo, da bi dobili tanke oksidne plasti na atomsko čistih površinah, smo jih oksidirali na dva načina. Vzorci so bili izpostavljeni ali atmosferi čistega kisika v pripravljalni komori pri tlaku 10^{-5} mbar in nato analizirani z XPS ali oksidirani v kisikovi plazmi pri temperaturah od 22 °C do 300 °C. Vse tanke plasti smo preučili z XPS- tehniko za določitev sestave oksidnih plasti na površini. Posebej smo nato pri večji energijski ločljivosti posneli še elemente za natančno določitev spreminjanja skozi oksidno plast, t. i. XPS-globinski profil. Ugotovili smo, da so nastale pri različnih pogojih različne oksidne plasti Fe/Cr različnih debelin v povezavi s temperaturo in načinom oksidacije. Opazili pa smo tudi, da je skoraj pri vseh temperaturah oksidacije ostal tudi delež neoksidiranih kovinskih elementov na površini.

Ključne beside: dupleksno nerjavno jeklo, oksidacija, plazemska oksidacija, XPS, nerjavno jeklo

1 INTRODUCTION

Stainless steel is one of the most widely used materials and has a large variety of applications. Therefore, it is exposed to a wide range of conditions. Since it is an alloy, various oxides can be formed on its surface, and they can change the mechanical, chemical and physical properties of the material. Steel's corrosion resistance originates in the Cr-rich oxide layer that acts as a barrier against ion diffusion between the alloy and the ambient phase.[1–4] Custom steel grades are designed for specific applications by optimizing their properties using specific alloy compositions. The study was on mass fractions 22 % chromium, 5–6 % nickel, 3 % molybdenum, 2 % manganese, nitrogen-alloyed duplex stainless steel (DSS 2205, also known as W.Nr. 1.4462), with high general, localized and stress corrosion resistance properties in addition to high strength and excellent impact toughness. Duplex stainless steels contain two equilibrium phases, i.e., ferrite and austenite. This type of stainless steel is increasingly used because of its several superior properties. It also has better corrosion resistance and erosion-fatigue properties as well as a lower thermal expansion coefficient and higher thermal conductivity than plain austenitic stainless steel. Its yield strength is about twice as high as that of austenitic stainless steels and this allows the designer to save material and makes the alloy more cost competitive in comparison to the 316L or 317L stainless steels. Alloy 2205 is particularly suitable for applications in the temperature interval from –50 °C to 300 °C. Temperatures outside this interval may also be considered, but there are some restrictions, particularly for welded structures.[5,6]

The oxidation and corrosion resistance of stainless steel has already been the subject of many studies. The corrosion resistance of stainless steel is known to be based on the Cr_2O_3 chromium oxide at the surface that is considered to act as a protective layer against corrosion due to its low diffusion constants for oxygen and metal ions.[7,8] The oxide layer formed on stainless-steel surfaces is usually not uniform in terms of the depth. Double or even triple layers can be formed on the surface, depending on the alloy composition, on the oxidizing conditions (oxidizing atmosphere, time, and temperature), and also on the different duplex stainless-steel iron phases.[9,10] Oxide films may theoretically consist of various iron and chromium oxides as well as their

mixtures. Several authors have studied the formation of thin oxide layers on stainless steels, being oxidized in air or oxygen at various pressures and various temperatures. The oxidation in air showed that at most temperatures a duplex oxide layer was formed; the outer layer, α-Fe_2O_3, was formed on the top of the inner oxide layer, an iron-chromium oxide. Under reduced oxygen partial pressures a fine chromium-rich oxide grows through the iron oxide layer that was formed initially. At very low oxygen pressures (below 10^{-3} Pa) and temperatures above 350 °C, chromium predominates throughout the oxide layer [11–15]. At low temperatures, on the other hand, i.e., up to 400 °C, only iron oxide is formed on the surface of stainless steels. This is not true, however, for all the FeCr alloys. Hultquist et al. [16], e.g., reported that a significant fraction of oxidized Cr was detected by the X-ray photoelectron spectroscopy (XPS) of FeCr alloys that were exposed to air at temperatures between 25 °C and 180 °C.

The aim of the present study was to examine the initial phases of oxide growth on the 2205 duplex stainless steel as a function of temperatures up to 300 °C. The oxide layers were produced by the controlled exposure of polished duplex stainless-steel samples to oxygen atoms. X-ray photoelectron spectroscopy (XPS) was applied to measure the depth distributions of the oxide films formed on the surface by the sputter depth profiling. To our knowledge, this is the first report on the depth distribution of oxide-layer compositions on DSS 2205 for the conditions specified in this paper. The results of an ongoing study of the oxidation in air will be described in a subsequent paper.

2 EXPERIMENTAL

Duplex 2205 stainless steel (DSS) was obtained from the Acroni, d. o. o., steel plant, which certified the alloy as 2205 duplex stainless steel with the composition as given in **Table 1**.[2]

The samples were mounted in resin, ground with emery papers up to No. 4000, and then polished with 1-μm diamond paste. Metallographic samples of approximately (8 × 8 × 1) mm were thus prepared. These samples were then mounted onto sample holders for the XPS examinations, using UHV-compatible double-sided sticky tape.

The oxidation was achieved in an experimental reactor for the passivation of metals. The reactor was a glass tube with a length of 40 cm and a diameter of 4 cm. It was evacuated from one side with a two–stage rotary pump with a pumping rate of 16 m^3h^{-1}. The ultimate pressure in the system was about 4 Pa and the residual atmosphere consisted mainly of water vapour. The other end of the reactor was connected to a source of neutral oxygen atoms. The source was a low-pressure oxygen plasma created by an inductively coupled RF generator operating at a frequency of 27.12 MHz and with a variable output power. The applied experimental procedure is described in detail elsewhere.[17–22] In our case the RF power was fixed at about 250 W. The plasma was characterized with a double Langmuir probe and a Fibre Optics Catalytic Probe (FOCP).[17,21,23,24] The Langmuir probe was placed in the centre of the plasma. At the applied pressure of 75 Pa the electron temperature was about 4 eV, while the electron density was about $7 \cdot 10^{15}$ m^{-3}. The FOCP was mounted in the experimental reactor for the passivation of metals close to the samples.[24] At a pressure of 75 Pa the O-atom density reached its peak value of about $1 \cdot 10^{22}$ m^{-3}. The neutral gas kinetics temperature in the passivation reactor was close to room temperature.

The samples were mounted on a heatable holder, heated to the appropriate temperature and kept in the passivation reactor for 100 s. In this period they received a dose of neutral oxygen atoms of about $1.5 \cdot 10^{24}$ m^2.

The XPS depth profiles of the oxide layers were measured with a VG Microlab 310F AES/SEM/XPS. Mg K_α radiation at 1253.6 eV with an anode power of 200 W (the anode voltage was 12.5 kV and the emission current 16 mA) was applied in all the XPS measurements. A 3-keV, 1-μA Ar^+ ion beam scanned over an (8 × 8) mm area was applied for the sputter depth profiling with an incidence angle of 60° (measured with respect to the sample normal). The approximate sputtering rate under the conditions applied here was 1 nm/min for SiO_2. This was not inconsistent with some calibration measurements performed on metallic and oxide-type samples as well as with some reference data for the sputtering rates of Fe and Cr and their oxides.[13,25–29]

The spectra were acquired using the Avantage 3.41v software supplied by the manufacturer. CasaXPS software[30] was used to process the data. The XPS spectra were fitted to determine the different chemical states' contributions to the total peak intensity.

3 RESULTS AND DISCUSSION

Figure 1 shows high-resolution XPS scans of the Cr $2p_{3/2}$ and Fe $2p_{3/2}$ transitions with the corresponding metallic and oxide components before sputtering the DSS 2205 that was prepared at 22 °C. In the case of Cr $2p_{3/2}$ four peaks were used for the fitting, i.e., the metallic peak and the three oxide peaks, CrO_3, Cr_2O_3 and $Cr(OH)_3$. The binding-energy differences of the compo-

Table 2: Chemical composition of the duplex stainless steel in mole fractions *x*/%

Cr	Ni	Mn	Si	P	S	C	Mo	N	Fe
23.96	4.82	1.48	0.85	0.05	0.00	0.13	1.83	0.67	66.21

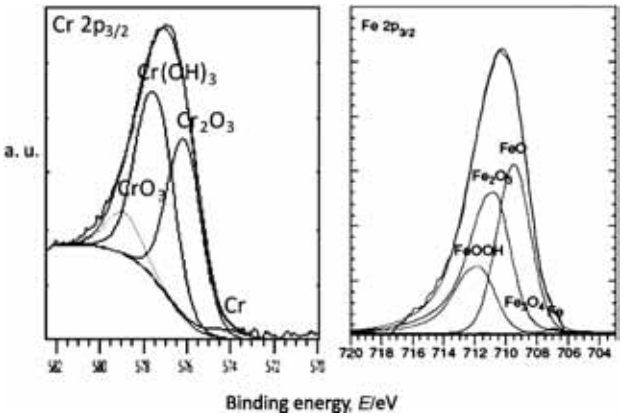

Figure 1: Examples of fitted Cr $2p_{3/2}$, Fe $2p_{3/2}$ XPS spectra
Slika 1: XPS-spektra Cr $2p_{3/2}$, Fe $2p_{3/2}$ z oksidnimi komponentami

nents were fixed at the values obtained from references [7,13,31,32] and the full widths at half maximum (FWHM) for the three oxide peaks were fixed to be the same. The FWHM applied for the metallic component was taken from the Cr peak, being measured after the surface oxides were removed. The expected presence of the three oxides was based on previous work. The Fe $2p_{3/2}$ was fitted with five peaks in a similar way.[6,26,33–39]

Figure 2 shows the Cr $2p_{3/2}$ and $2p_{1/2}$ transitions after various sputtering times for the sample prepared at 22 °C. At each depth the $2p_{3/2}$ peak was fitted as discussed above (see Figure 1). The total Cr oxide concentration was approximated by adding the areas of the three oxide-peak components. The intensities of the oxide components were reduced by sputtering and eventually only the metallic component remained. The Fe data were processed similarly.

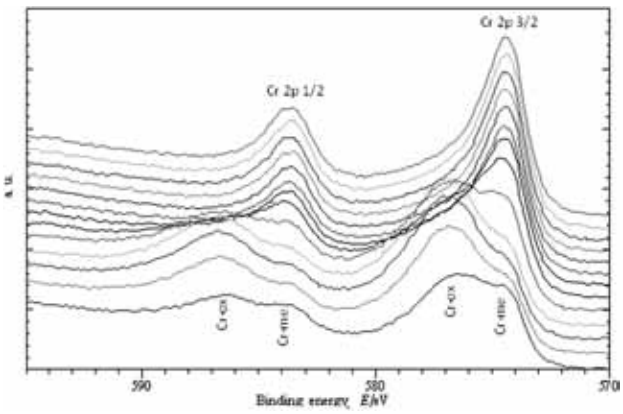

Figure 2: Set of high-resolution XPS spectra of Cr 2p transitions used for constructing the Cr depth profiles in **Figure 3**. The bottom spectrum is from the surface before sputtering, and the spectra above it belong to spots of increased depth from the original surface. The spectra have been offset in intensity for clarity.
Slika 2: Visoko ločljivi XPS-spektri Cr 2p vrha, ki smo jih uporabili za izdelavo globinskih profilov v XPS **sliki 3**. Spodnji spekter je na površini vzorca pred jedkanjem, zgornji spekter pa je po seriji jedkanj. Spektri so zamaknjeni po intenziteti za boljši pregled.

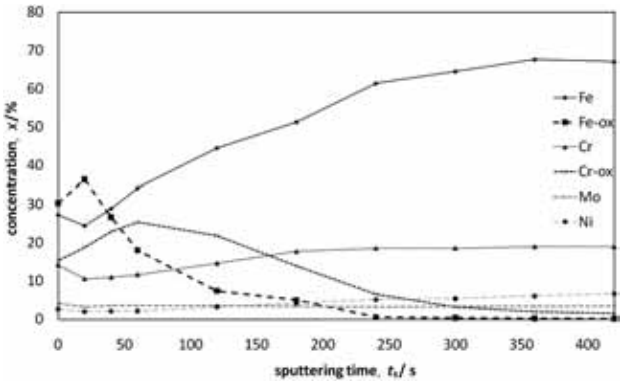

Figure 3: XPS depth profile of DSS at 200 L exposure in the preparation chamber
Slika 3: XPS; globinski profil DSS pri izpostavljenosti 200 L v pripravljalni komori

Figure 3 shows an XPS depth profile of the oxide layer after the oxidation of the DSS 2205 with an exposure to 200 L (Langmuir) of oxygen in the preparation chamber. The stoichiometry of the oxide was, in the best case, an approximation because of the ion-sputtering-induced effects, such as the reduction of the oxidation state.

XPS depth profiles were also measured with the DSS 2205 after much longer exposures to oxygen, i.e., up to 8000 L (**Figure 4**), without obtaining substantially different results. This suggested that an increase in the pressure and/or different atmospheric conditions, e.g., humidity, were needed to produce a thicker oxide layer.

The profiles in **Figures 3 and 4** showed that these oxide layers were ill-defined with slowly changing concentrations of oxidized and unoxidized metals from the surface of the oxide layer towards the interior of the sample. Also, large fractions of unoxidized metals were present at the very surface of the oxide layers. These concentrations might be partially overestimated since the estimations of oxide-layer thicknesses obtained from the profiles in **Figures 3 and 4** were 2–3 nm, i.e., of the order of the probing depth of the applied XPS in the

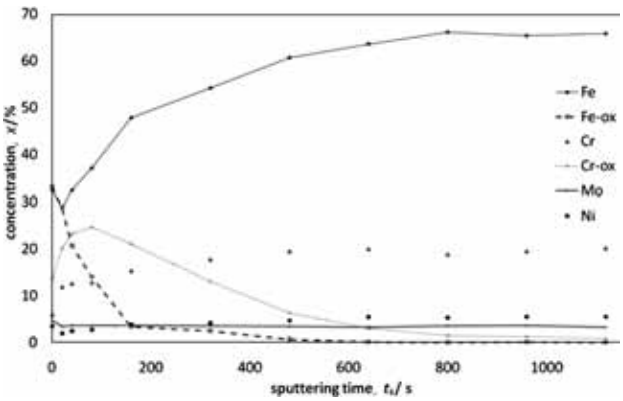

Figure 4: XPS depth profile of DSS at 8000 L exposure in the preparation chamber
Slika 4: XPS; globinski profil DSS pri izpostavljenosti 8000 L v pripravljalni komori

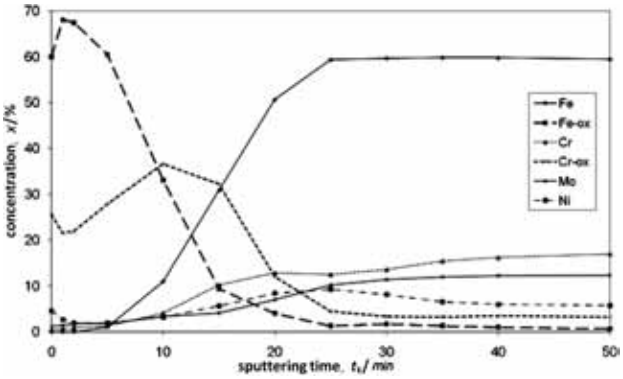

Figure 5: XPS depth profile of DSS oxidized at 22 °C
Slika 5: XPS; globinski profil DSS po oksidaciji v plazmi pri 22 °C

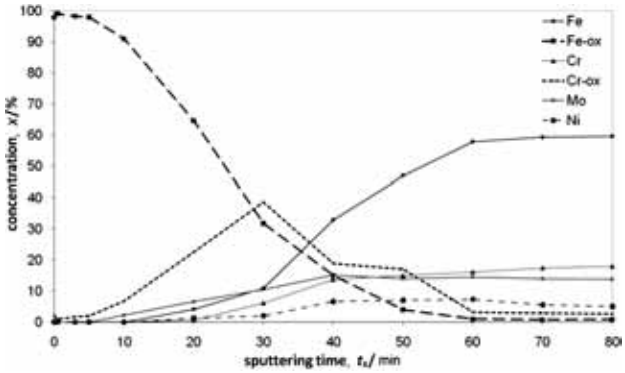

Figure 7: XPS depth profile of DSS oxidized at 300 °C
Slika 7: XPS; globinski profil DSS po oksidaciji v plazmi pri 300 °C

analysis, so there existed some possibility that unoxidized metals from the bulk influenced the measurements. Even in those poorly defined oxide layers, two-oxide structures could already be detected: a higher concentration of iron oxide at, and close to, the surface, with chromium oxide being the predominant oxide at greater depths, in contrast to the layer of the bulk interface.

The stoichiometry of the oxide was, in the best case, an approximation due to ion-sputtering-induced effects, such as the reduction of the oxidation states.[16,27,28,40] However, valid comparisons could be made between the relative oxidation degrees at various temperatures. The formation of an oxide film with an inner region, essentially consisting of chromium oxide, and an outer region, mainly consisting of iron oxide, was also observed in the samples that were heated up to 300 °C. A. P. Greeff et al.[41] found that the formation of Fe_2O_3 on the FeCrMo steel was, in the interval between room temperature and 300 °C, more rapid than that of the initially formed Cr_2O_3, and it was eventually formed on the top of the Cr-oxide. This is in agreement with our results. The concentration of the unoxidized metallic species in the topmost part of the oxide layer was much lower than the concentration of their oxidized counterparts, while there was virtually no unoxidized chromium or iron in the oxide layer. **Figure 6** shows a different metal-oxide distribution for the sample that was oxidized at a higher temperature of 150 °C (423 K). The concentration of iron oxides close to the surface was, in this case, much higher than that in the sample oxidized at 22 °C (**Figure 5**), being about mole fraction x = 85 % compared to the previous value of about mole fraction of x = 70 %, and it showed the segregation of iron oxides at the surface. On the other hand, the concentration of chromium oxides was about x = 10 %, compared to x = 25 %, showing the reduced surface segregation of Cr (oxides) at 150 °C . The thickness of the oxide layer was also somewhat greater than that formed with plasma oxidation at room temperature and very much thicker than that formed with just pure oxygen. In both cases, the amount of chromium oxides increased at the interface between the surface oxides and the underlying steel. **Figure 7** shows the XPS depth profile of DSS oxidized at 300 °C (573 K). The further increase of iron oxides and the further reduction of chromium oxides in the oxide film were quite dramatic compared to the depth profiles of the samples being oxidized at lower temperatures, as well as the increased thickness of the oxide layer itself. Other effects observed in the sputter depth profiles at 22 °C and 150 °C (**Figures 5 and 6**) remained unchanged, i.e., the increased concentration of chromium oxides at the interface of the oxide layer and steel substrate. A comparison of **Figures 5, 6 and 7** makes it clear that the total oxide layer was thicker, and the ratio of the iron oxides to chromium oxides increased with increasing oxidation temperature (up to 300 °C). However, it was observed that the amount of chromium oxides increased at the interface of the surface oxide layers and substrate to approximately $x \approx 35$ % in all cases. It is known, as a general rule, that iron oxide is the predominant surface oxide in stainless steels at temperatures up to 400 °C,[9] and this research showed the actual temperature dependence of this predominant species within the mentioned temperature range. The composition and oxidation behaviour of the various grains was known to be very similar, and the XPS analysis was made on a 1 mm × 2 mm area that was much greater than the grain size.

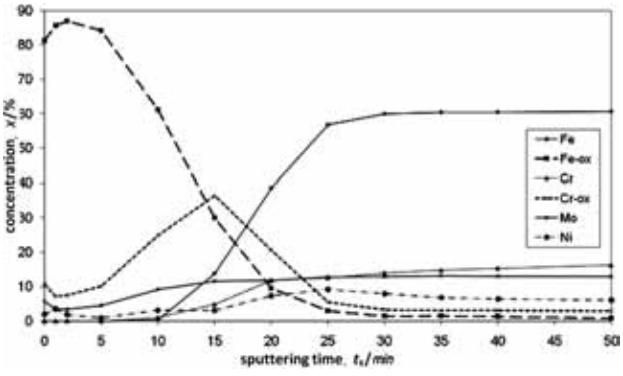

Figure 6: XPS depth profile of DSS oxidized at 150 °C
Slika 6: XPS; globinski profil DSS po oksidaciji v plazmi pri 150 °C

An enrichment with Mo throughout the oxide layer was observed at all temperatures. The oxide layer of DSS had a duplex structure of Fe oxides, predominantly Fe_2O_3, on the outer side and Cr oxides, predominantly Cr_2O_3, on the inner side of layer, with an enrichment of Mo underneath the Cr oxide layer. This enrichment of Mo might be explained by the assumption that Mo oxidizes less readily than Fe or Cr. The Gibbs free energies for the formation of Fe_2O_3, Cr_2O_3 and MoO_3 at 700 K (427 °C) are – 979 J/mol, – 1209 J/mol and – 799 J/mol, respectively, and they correspond to – 744,8 J/mol, – 807,5 J/mol and – 535,5 J/mol O_2. From the viewpoint of thermodynamics, the oxidation of Mo is the least favourable. Furthermore, according to Mathieu and Landolt [5], the presence of Mo at the oxide/metal interface could influence the oxide growth in two ways: Mo could reduce the activity of Fe at the phase boundary or it could form a diffusion barrier for Fe and Cr ions between the oxide and the metal.

In summary, the oxidation of DSS 2205 with atomic oxygen revealed two important factors that influenced the growth and composition of the oxide layers that were formed at various temperatures, i.e., the segregation of the alloying elements to the surface and the influence of atomic oxygen on the oxidation process.

4 CONCLUSIONS

Two different types of oxide layers were obtained. The first one was very thin, of the order of 2–5 nm, obtained with exposure to oxygen at 10^{-5} mbar, independent of the total exposure time, even when the exposure times differed by two orders of magnitude. The second one was of the order of a few tenths of nm, obtained by exposure to plasma oxidation, also at higher temperatures. A more detailed analysis showed that despite the great similarities between the samples that were oxidized either with oxygen or with plasma there were also differences in certain numerical parameters (e.g., the ratios of unoxidized versus oxidized iron, or metal in general) that allowed us to denote the plasma-oxidized sample as a more "thoroughly" oxidized. A common characteristic of all the examined layers was a double-oxide stratification, with the regions closer to the surface that contained higher concentrations of iron oxide, and those more towards the interior, exhibiting higher concentrations of chromium oxide. The compositions of the oxide films formed on the DSS 2205 by exposure to plasma oxygen atoms are presented from room temperature to 300 °C. Different oxide layers were formed on the surface, depending on the temperature during the atomic oxidation. Small increments of temperature above room temperature resulted in increased amounts of Fe oxides and reduced amounts of Cr oxides on the surface, while almost pure Fe oxides were formed at 300 °C. There was an enrichment of chromium oxides at the interface between the surface oxide and the bulk material at all the temperatures. Due to this Cr enrichment at the interface, the upper part of the bulk material consisted of the so-called chromium-depleted layer. This study also provided important results about the behaviour of the DSS 2205 that was treated with oxygen atoms from relatively low temperatures up to just 300 °C. To examine this advanced exposure a chamber with the possibility of increasing the exposure pressure, measured in mbars, could be used. Another possibility for further studies is to use ARXPS for more accurate depth profiling of the thinnest oxide layers.

5 REFERENCES

[1] G. Betz, G. K. Wehner, L. Toth, Journal of Applied Physics 45 (**1974**), 5312–5316

[2] ASM specialty handbook: Stainless Steels, 1996, 32–34

[3] M. Veljkovic, J. Gozzi, Journal of Pressure Vessel Technology-Transactions of the ASME 2007, 129, 155–161 10.1115/1.2389034

[4] S. Ohkido, Y. Ishikawa, T. Yoshimura, POSAP analysis of the oxide alloy interface in stainless-steel, 1994, Chapter, 261–265

[5] H. J. Mathieu, D. Landolt, Corrosion Science 26 (**1986**), 547–559

[6] C. Palacio, H. J. Mathieu, V. Stambouli, D. Landolt, Surface Science 295 (**1993**), 251–262

[7] C. M. Abreu, M. J. Cristobal, X. R. Novoa, G. Pena, M. C. Perez, Surface and Interface Analysis 2008, 40, 294–298 10.1002/sia.2796

[8] H. Asteman, K. Segerdahl, J. E. Svensson, L. G. Johansson, M. Halvarsson, J. E. Tang, p. trans tech, In: Oxidation of stainless steel in H2O/O-2 environments – Role of chromium evaporation, 2004, Chapter, 775–782

[9] A. Vesel, A. Drenik, M. Mozetic, A. Zalar, M. Balat-Pichelin, M. Bele, In: AES investigation of the stainless steel surface oxidized in plasma, 2007, Chapter, 228–231

[10] A. Vesel, M. Mozetic, A. Drenik, N. Hauptman, M. Balat-Pichelin, Applied Surface Science 255 (**2008**), 1759–1765 10.1016/j.apsusc.2008.06.017

[11] Y. Ishikawa, K. Odaka, Reduction of outgassing from stainless surfaces by surface oxidation, 1990, Chapter, 1995–1997

[12] Y. Ishikawa, T. Yoshimura, Journal of Vacuum Science & Technology a-Vacuum Surfaces and Films 13 (**1995**), 1847–1852

[13] A. Kocijan, C. Donik, M. Jenko, Corrosion Science 49 (**2007**), 2083-2098 10.1016/j.corsci.2006.11.001

[14] S. Shibagaki, A. Koga, Y. Shirakawa, H. Onishi, H. Yokokawa, J. Tanaka, Thin Solid Films 303 (**1997**), 101–106

[15] G. J. Stokkers, A. Vansilfhout, G. A. Bootsma, T. Fransen, P. J. Gellings, Corrosion Science 23 (**1983**), 195–204

[16] G. Hultquist, M. Seo, N. Sato, Oxidation of Metals 25 (**1986**), 363–372

[17] U. Cvelbar, M. Mozetic, A. Ricard, Characterization of oxygen plasma with a fiber optic catalytic probe and determination of recombination coefficients, ed. by Editor, City, 2005, Chapter, 834–837

[18] U. Cvelbar, M. Mozetic, Journal of Physics D-Applied Physics 2007, 40, 2300–2303 10.1088/0022–3727/40/8/s09

[19] U. Cvelbar, K. Ostrikov, A. Drenik, M. Mozetic, Applied Physics Letters 92 (**2008**), 133505 10.1063/1.2905265

[20] A. Drenik, U. Cvelbar, K. Ostrikov, M. Mozetic, Journal of Physics D-Applied Physics 41 (**2008**), 115201 10.1088/0022-3727/41/11/115201

[21] M. Mozetic, A. Zalar, U. Cvelbar, D. Babic, AES characterization of thin oxide films growing on Al foil during oxygen plasma treatment, 2004, Chapter, 986–988

[22] M. Mozetic, U. Cvelbar, A. Vesel, N. Krstulovic, S. Milosevic, Ieee Transactions on Plasma Science 36 (**2008**), 868–869 10.1109/tps.2008.925383

[23] U. Cvelbar, M. Mozetic, I. Poberaj, D. Babib, A. Ricard, Characterization of hydrogen plasma with a fiber optics catalytic probe, 2005, 12–16
[24] M. Mozetic, Characterization of reactive plasmas with catalytic probes, 2007, Chapter, 4837–4842
[25] J. R. Lince, S. V. Didziulis, D. K. Shuh, T. D. Durbin, J. A. Yarmoff, Surface Science 277 (**1992**), 43–63
[26] D. Mandrino, M. Godec, M. Torkar, M. Jenko, Surface and Interface Analysis 40 (**2008**), 285–289 10.1002/sia.2718
[27] N. S. McIntyre, F. W. Stanchell, Journal of Vacuum Science & Technology 16 (**1979**), 798–802
[28] A. Zalar, Thin Solid Films 124 (**1985**), 223–230
[29] A. Kocijan, I. Milosev, D. K. Merl, B. Pihlar, Journal of Applied Electrochemistry 34 (**2004**), 517–524
[30] N. Fairley, http://www.casaxps.com/
[31] A. Maetaki, M. Yamamoto, H. Matsumoto, K. Kishi, Surface Science 445 (**2000**), 80–88
[32] A. Kocijan, I. Milosev, B. Pihlar, Journal of Materials Science-Materials in Medicine 15 (**2004**), 643–650
[33] Dj. Mandrino, M. Jenko A study of oxide layers on electrical steels prepared with different thermal treatments, 2001, Chapter, 157–161
[34] Dj. Mandrino, M. Godec, P. Skraba, B. Sustarsic, M. Jenko, AES, XPS and EDS analyses of an iron-based magnetic powder and an SMC material, 2004, Chapter, 912–916
[35] Dj. Mandrino, M. Lamut, M. Godec, M. Torkar, M. Jenko, Surface and Interface Analysis 39 (**2007**), 438–444 10.1002/sia.2534
[36] J. Baltrusaitis, D. M. Cwiertny, V. H. Grassian, Physical Chemistry Chemical Physics 9 (**2007**), 5542–5554 10.1039/b709167b
[37] C. R. Brundle, T. J. Chuang, K. Wandelt, Surface Science 68 (**1977**), 459–468
[38] A. P. Grosvenor, B. A. Kobe, M. C. Biesinger, N. S. McIntyre, Surface and Interface Analysis 36 (**2004**), 1564–1574 10.1002/sia.1984
[39] E. Paparazzo, Journal of Electron Spectroscopy and Related Phenomena 154 (**2006**), 38–40 10.1016/j.elspec.2006.09.004
[40] C. Leygraf, G. Hultquist, Surface Science 61 (**1976**), 69–84
[41] A. P. Greeff, C. W. Louw, H. C. Swart, Corrosion Science 42 (**2000**), 1725–1740